International Journal of Multiphase Flow 34 (2008) 678–683

Contents lists available at ScienceDirect

International Journal of Multiphase Flow

journal homepage: www.elsevier.com/locate/ijmulflow

On the orientation of ellipsoidal particles in a turbulent shear flow

P.H. Mortensen [a,*], H.I. Andersson [a], J.J.J. Gillissen [b], B.J. Boersma [b]

[a] Department of Energy and Process Engineering, Norwegian University of Science and Technology, Norway
[b] Laboratory for Aero and Hydrodynamics, TU-Delft, The Netherlands

ARTICLE INFO

Article history:
Received 4 June 2007
Received in revised form 15 October 2007

Keywords:
Ellipsoids
Orientation
Turbulence

ABSTRACT

Direct numerical simulation (DNS) of small prolate ellipsoidal particles suspended in a turbulent channel flow is reported. The coupling between the fluid and the particles is one-way. The particles are subjected to the hydrodynamic drag force and torque valid for creeping flow conditions. Six different particle cases with varying particle aspect ratios and equivalent response times are investigated. Results show that, in the near-wall region, ellipsoidal particles tend to align with the mean flow direction, and the alignment increases with increasing particle aspect ratio. When the particle inertia increases, the particles are less oriented in the spanwise direction and more oriented in the wall-normal direction. In the core region of the channel, the orientation becomes isotropic.

1. Introduction

The suspension of small elongated particles in a turbulent stream occurs in several industrial applications and environmental phenomena, such as transportation of particles in pipes and channels, separation in cyclones, sediment transport in rivers and dispersion of small particles in the atmosphere. Most of the research on particulate flows considers spherical particles. This is often due to the isotropic nature of the sphere which makes it much easier to represent both mathematically and numerically. Since a sphere is isotropic, its orientation is immaterial, and the translational motion can be solved independently of the rotational motion. On the other hand, for elongated particles the orientation must be considered since it influences the translational motion.

Even though most of the literature considers spherical particles (see for instance Marchioli et al. (2007), Kuerten (2006) and Kulick et al. (1994)), the study of elongated particles immersed in a viscous fluid has been a subject for research through several decades. There exist several analytical studies on elongated (ellipsoidal) particles, see for instance Jeffery (1922), Brenner (1963, 1964) and Harper and Chang (1968). Also, the literature reports both numerical and experimental work on elongated particle or fiber suspensions, such as Fan and Ahmadi (1995), Newsom and Bruce (1994, 1998), Zhang et al. (2001), Lin et al. (2003) and Parsheh et al. (2005) to name a few. Newsom and Bruce (1998) studied the orientational behavior of fibrous aerosols in atmospheric turbulence both experimentally and numerically and found that fibers exhibited a tendency for horizontal orientation. Also, they found that the orientational preference was more sensitive to fiber diameter than to length. Zhang et al. (2001) numerically investigated the motion of ellipsoidal particles in a turbulent channel flow. They reported the orientational statistics for ellipsoidal particles of aspect ratio 5 and equivalent response time $\tau^+ = 5$ in the near-wall region. They found that the particles oriented in the streamwise direction.

The purpose of the present paper is to study how small inertial prolate ellipsoids orient in a turbulent shear flow. This study is complementary to that by Zhang et al. (2001) and the effects of aspect ratio and particle inertia will be reported. It is assumed that the particles are smaller than the Kolmogorov scale of turbulence for a frictional Reynolds number of 360. Further it is assumed that the flow field in the immediate neighborhood of the particles is locally Stokesian. The ellipsoids are subjected to hydrodynamic drag force and torque (Jeffery, 1922). The coupling between the particles and fluid is one-way, i.e., the flow field only acts on the particles.

2. Eulerian fluid dynamics

The incompressible, isothermal and Newtonian fluid into which the particles are released is governed by the continuity and the Navier–Stokes equation

$$\nabla \cdot \mathbf{u} = 0, \tag{1}$$

$$\frac{\partial \mathbf{u}}{\partial t} + (\mathbf{u} \cdot \nabla)\mathbf{u} = -\nabla p + Re_*^{-1}\nabla^2 \mathbf{u}. \tag{2}$$

In the equations above, $\mathbf{u} = \langle u_x, u_y, u_z \rangle$ is the fluid velocity vector, p is the pressure and $Re_* = u_* h/\nu$ is the frictional Reynolds number based

* Corresponding author. Tel.: +47 73593564.
E-mail address: paal.h.mortensen@ntnu.no (P.H. Mortensen).

0301-9322/$ - see front matter © 2008 Elsevier Ltd. All rights reserved.
doi:10.1016/j.ijmultiphaseflow.2007.12.007

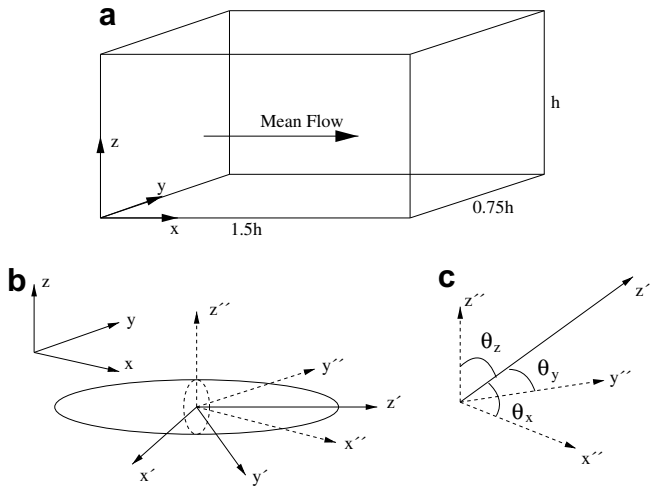

Fig. 1. (a) Computational domain, (b) Cartesian coordinate systems; inertial frame $\mathbf{x}$, particle frame $\mathbf{x}'$ and co-moving frame $\mathbf{x}''$, and (c) Orientational angles of an ellipsoid with semi-major axis z'.

upon the friction velocity u^*, channel height h and kinematic viscosity ν.

A direct numerical simulation is used to solve the fluid equations of motion (Eqs. (1) and (2)) at a frictional Reynolds number $Re^* = 360$. The size of the computational domain is $1.5h$ in the streamwise direction, $0.75h$ in the spanwise direction and h in the wall-normal direction, see Fig. 1(a). Periodic boundary conditions are applied in the streamwise (x) and spanwise (y) directions, respectively. In the wall-normal direction (z), no-slip conditions are enforced at both walls ($z = 0$ and $z = h$). The computations are carried out with $48 \times 48 \times 192$ gridpoints in the x, y and z directions, respectively. In the wall-normal direction the grid is slightly refined towards the wall such that Δz^+ varies between 0.9 and 2.86 wall-units. The resolution in the homogeneous directions is $\Delta x^+ = 11.3$ and $\Delta y^+ = 5.6$. The timestep is $\Delta t^+ = 0.036$ in wall-units. The same algorithm as that used by Gillissen et al. (2007) is employed for solving the fluid equations of motion.

3. Lagrangian particle dynamics

The mathematical description of small inertial prolate ellipsoidal particles suspended in a viscous shear flow is given in Zhang et al. (2001) and Gallily and Cohen (1979). In this paper, the particles will be treated in the same fashion. Below, a short description of the Lagrangian particle dynamics is given. The interested reader is referred to Zhang et al. (2001) for a more detailed description.

In order to describe the general motion of prolate ellipsoids it is convenient to invoke three different Cartesian coordinate systems: the inertial frame, the particle frame and the co-moving frame. The inertial frame, $\mathbf{x} = \langle x,y,z\rangle$, is the frame that spans the computational domain. The particle frame, $\mathbf{x}' = \langle x',y',z'\rangle$, is attached to the particle with origin at the particle mass-center. The coordinate axes are aligned with the principal directions of inertia. The co-moving frame, $\mathbf{x}'' = \langle x'',y'',z''\rangle$, is attached to the particle with origin at the mass-center of the particle. The coordinate axes are parallel to the inertial frame. The different coordinate systems are shown in Fig. 1(b). The purpose of introducing the co-moving system is to describe the orientational behavior of the ellipsoids. The particle orientation is important since it influences both the rotational and translational motion. The orientation of the particle frame relative to the co-moving frame is given by the nine direction cosines (Goldstein, 1980) which relate the same vector in two different coordinate systems through the linear transformation $\mathbf{x}' = \mathbf{A}\mathbf{x}''$, where the orthogonal transformation matrix $\mathbf{A}$ comprises the direction cosines.

The translational equation of motion is given by the linear momentum relation according to

$$m\frac{d\mathbf{v}}{dt} = \mathbf{F}. \tag{3}$$

Here, m is mass of the ellipsoid and $\mathbf{v} = \langle v_x, v_y, v_z\rangle$ is the velocity vector. The drag force $\mathbf{F}$ acting on an ellipsoid under creeping flow conditions is given by Brenner (1964)

$$\mathbf{F} = \mu\mathbf{A}^t\mathbf{K}'\mathbf{A}(\mathbf{u} - \mathbf{v}), \tag{4}$$

where $\mu = \rho\nu$ is the dynamic viscosity of the fluid and $\mathbf{K}'$ is the resistance tensor.

An important parameter is the particle response time, i.e., the time the particle needs to respond to changes in the flow field due to its inertia. For an ellipsoidal particle which is non-isotropic, the response time is not as obvious as for a spherical particle. Shapiro and Goldenberg (1993) defined an equivalent response time based upon isotropic particle orientation and the inverse of the resistance tensor. Zhang et al. (2001) presented their result in the form

$$\tau^+ = \frac{2\lambda D a^{+2}}{9}\frac{\ln(\lambda + \sqrt{\lambda^2 - 1})}{\sqrt{\lambda^2 - 1}}, \tag{5}$$

where D is the density ratio of particle to fluid and $\lambda = b/a$ is the aspect ratio where a is the semi-minor axis and b is the semi-major axis of the ellipsoid. The superscript "+" indicates that the parameters are scaled with viscous units ν and u_*.

The rotational motion of the ellipsoids is given by the Euler equations (Goldstein, 1980)

$$I'_{xx}\frac{d\omega'_x}{dt} - \omega'_y\omega'_z(I'_{yy} - I'_{zz}) = N'_x, \tag{6}$$

$$I'_{yy}\frac{d\omega'_y}{dt} - \omega'_z\omega'_x(I'_{zz} - I'_{xx}) = N'_y, \tag{7}$$

$$I'_{zz}\frac{d\omega'_z}{dt} - \omega'_x\omega'_y(I'_{xx} - I'_{yy}) = N'_z, \tag{8}$$

where ω'_x, ω'_y and ω'_z are the components of the angular velocity vector, I'_{xx}, I'_{yy} and I'_{zz} are the principle moments of inertia, respectively. The right hand sides of the equations above are the Jeffery torque components, Jeffery (1922). Notice that the Euler equations are solved in the particle frame. In addition to the linear and angular momentum relations, differential equations for particle positions and particle orientations are solved.

The particle translational and rotational equations of motion (Eqs. (3) and (6)–(8)) are solved by a mixed differencing procedure (Fan and Ahmadi, 1995). Time integrations of particle positions and orientations are made with a second order Adams–Bashforth scheme. The time step used in the particle equations is the same as that used for the Navier–Stokes equations. The particles are released randomly in the computational domain with random orientations. The initial particle velocities equal the corresponding fluid

Table 1
Particle parameters for the six different cases

Case	λ	D	τ^+	N
F10	10	23	0.5	20,000
F30	30	152	0.5	20,000
F50	50	377	0.5	20,000
S10	10	463	10	20,000
S30	30	3052	10	20,000
S50	50	7539	10	20,000

velocities at the particle positions. The particle boundary conditions are periodic in the two homogeneous directions. If a particle hits the wall, it is re-introduced randomly into the computational domain.

4. Results and discussion

In the present study, six different particle sets are investigated, see Table 1. In all cases, the number of particles N is kept

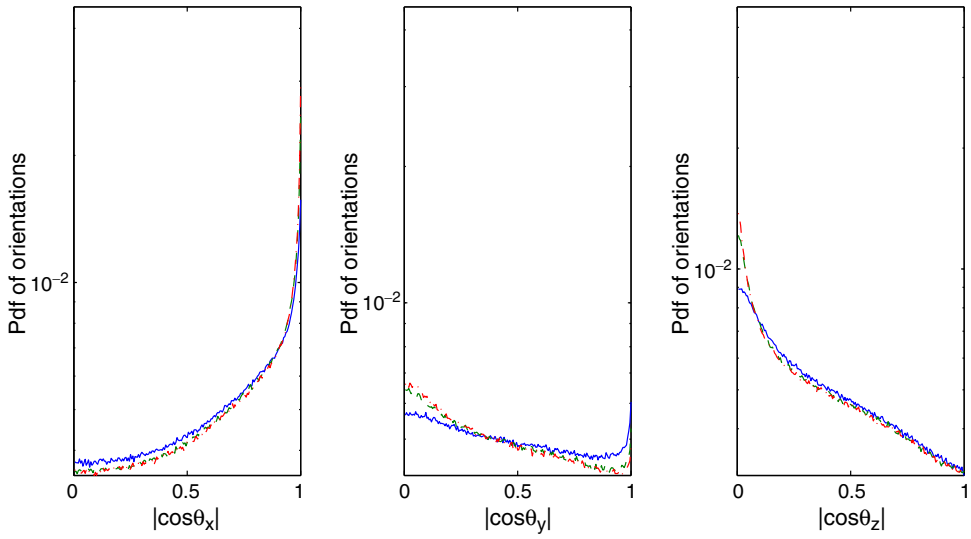

Fig. 2. Pdf of particle orientations. Streamwise orientation (left), spanwise orientation (middle), wall-normal orientation (right); (—) Case F10, (--) Case F30, (-·-) Case F50.

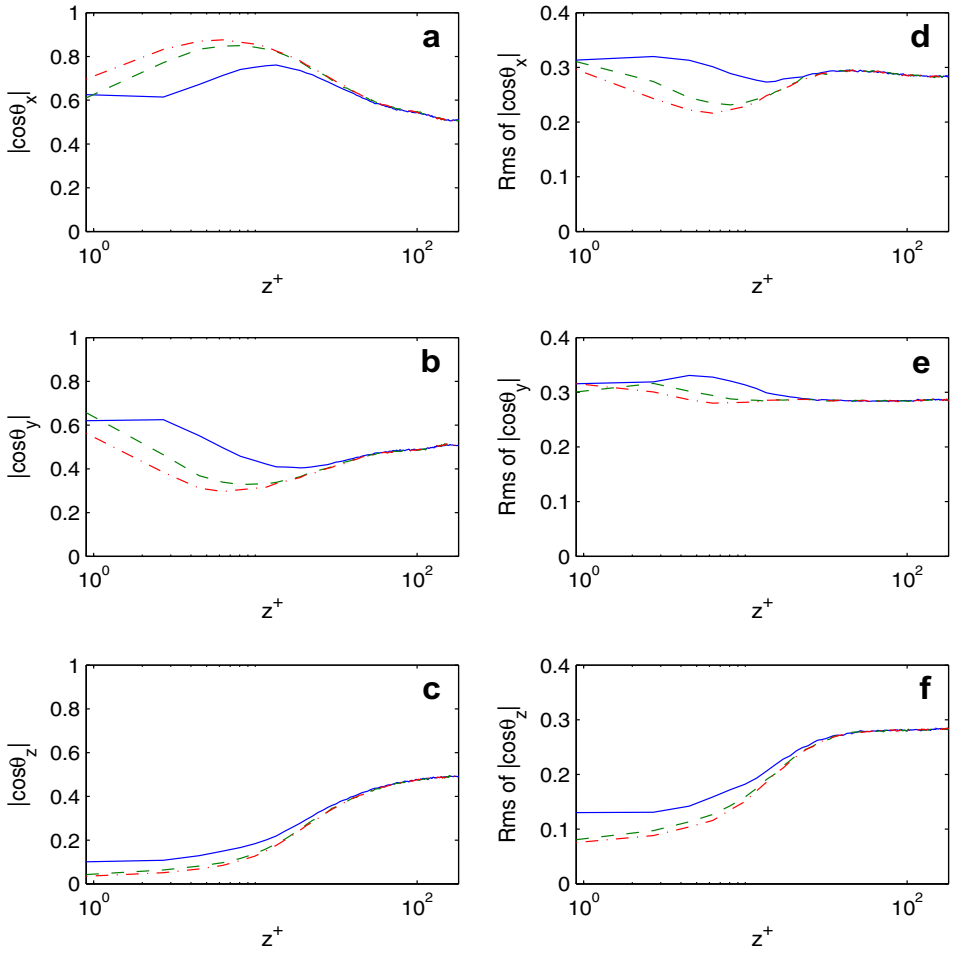

Fig. 3. Mean and rms values of direction cosines for ellipsoids with equivalent response time $\tau^+ = 0.5$; (—) Case F10, (--) Case F30, (-·-) Case F50. (a) $|\cos\theta_x|$, (b) $|\cos\theta_y|$, (c) $|\cos\theta_z|$, (d) $|\cos\theta_x|_{rms}$, (e) $|\cos\theta_y|_{rms}$, and (f) $|\cos\theta_z|_{rms}$.

constant. The density ratio D is varied in order to fix the response times for different aspect ratios. The results will focus on the orientation of the ellipsoids, where the orientation is described by the three angles (or direction cosines) the ellipsoids semi-major axis makes with the axes of the co-moving system, see Fig. 1(c).

4.1. Ellipsoids with equivalent response time $\tau^+ = 0.5$

The probability density function of particle orientations (mean direction cosines) is shown in Fig. 2. It is seen that the particles have large probability of orientation in the streamwise direction and lower probability of being oriented in the spanwise and

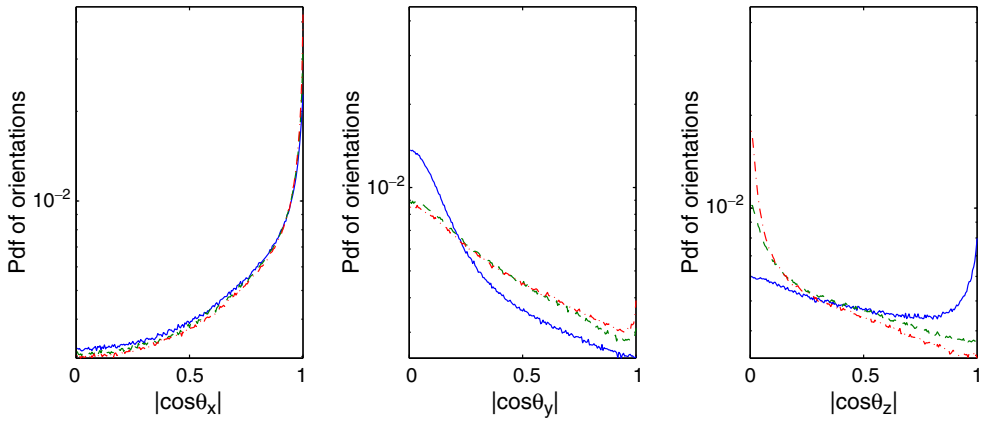

Fig. 4. Pdf of particle orientations. Streamwise orientation (left), spanwise orientation (middle), wall-normal orientation (right); (—) Case S10, (- -) Case S30, (-·-) Case S50.

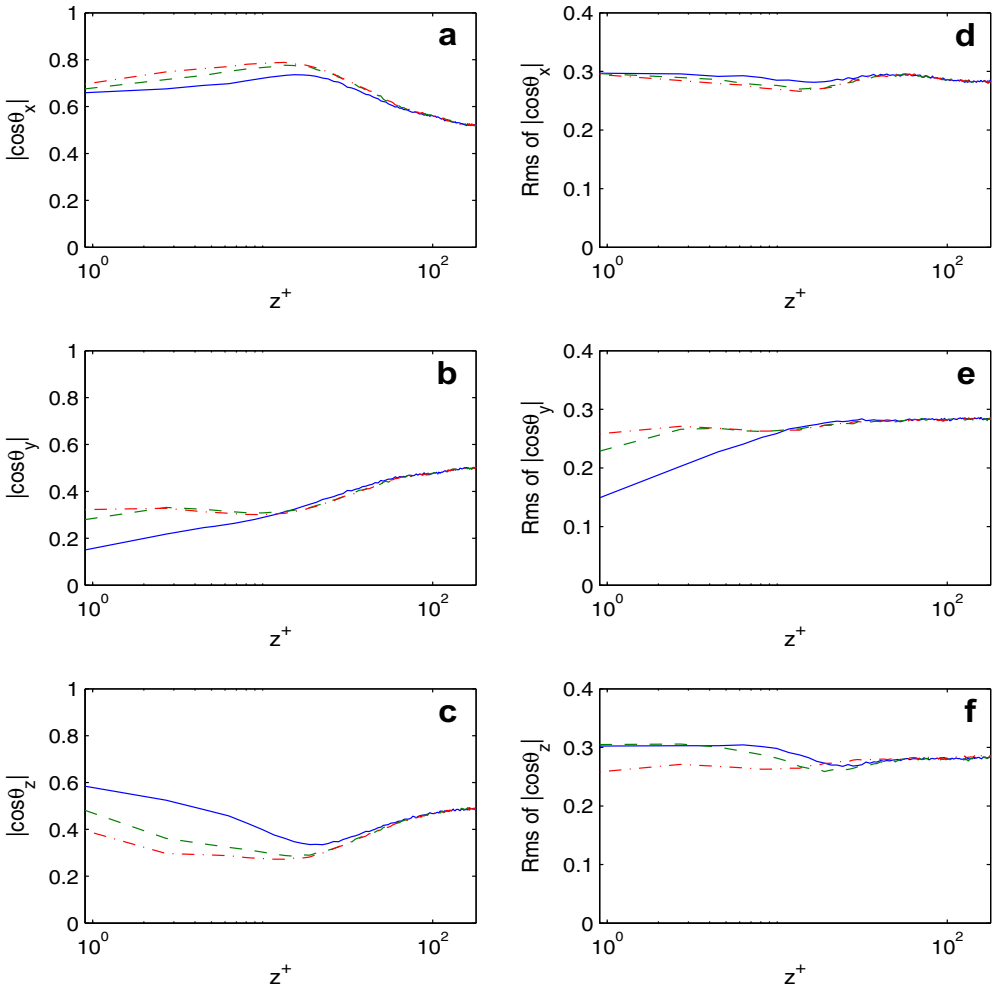

Fig. 5. Mean and rms values of direction cosines for ellipsoids with equivalent response time $\tau^+ = 10$; (—) Case S10, (- -) Case S30, (-·-) Case S50. (a) $|\cos\theta_x|$, (b) $|\cos\theta_y|$, (c) $|\cos\theta_z|$, (d) $|\cos\theta_x|_{\mathrm{rms}}$, (e) $|\cos\theta_y|_{\mathrm{rms}}$, and (f) $|\cos\theta_z|_{\mathrm{rms}}$.

wall-normal direction. These probabilities become more pronounced with increased aspect ratio λ.

Fig. 3(a)–(c) shows the mean orientations of the ellipsoids relative to x, y and z directions, respectively. It is seen that particles achieve increasing orientation in the streamwise direction in the near-wall region with increasing aspect ratio. Also, it is noted that the peak is shifted towards the wall with increasing aspect ratio. The opposite trend is seen for the spanwise orientation (Fig. 3(b)), in which direction the particles seem to be less oriented with increasing aspect ratio. The wall-normal orientation is shown in Fig. 3(c). In the core of the channel, the particles are oriented towards the wall while they are more aligned with the wall in the near-wall region. In the near-wall layer, the streamwise turbulent fluctuations dominate the spanwise and wall-normal fluctuations. It is possible that the net effect of the fluctuations is to stabilize the ellipsoids such that they mostly orient in the streamwise direction due to the dominating streamwise turbulent intensity. Also, since the particles mainly rotate about the y'' axis (not shown here), they will spend most of their time oriented in the streamwise direction. When the aspect ratio increases, the moment of inertia about the two semi-minor axes becomes larger. Hence, the effect is that the ellipsoids have larger probability of being oriented in the streamwise direction with increasing aspect ratio. In the core region of the channel, where the turbulent fluctuations are nearly isotropic, the orientation also becomes isotropic. The particles do not seem to preferentially orient in a specific direction.

The fluctuations of the particle orientations are shown in Fig. 3(d)–(f). Away from the wall ($z^+ > 40$) the fluctuations become isotropic. In the near-wall region, the orientational fluctuations dominate in streamwise and spanwise directions while they are less prominent in the wall-normal directions.

4.2. Ellipsoids with equivalent response time $\tau^+ = 10$

Fig. 4 shows the probability of orientation for ellipsoids with equivalent response time $\tau^+ = 10$. Also here it is seen that the particles have larger probability of orienting in the streamwise direction and this tendency increases with aspect ratio. It is interesting to see that case S10 particles behave quite differently than S30 and S50 particles. Comparing case F10 and case S10 it is seen that F10 particles have larger probability of being oriented in the spanwise direction. Also, S10 particles seem to be more oriented in the wall-normal direction.

The absolute value of the mean direction cosines for ellipsoids with equivalent response time $\tau^+ = 10$ is shown in Fig. 5(a)–(c). Comparing with Fig. 3, the effect of particle inertia is important for the orientations. In this case, also here the particles seem to preferentially orient in the streamwise direction in the near-wall region. This tendency increases with particle aspect ratio. On the other hand, the particles seem to be less oriented in the spanwise direction as compared to Fig. 3 and less aligned with the wall. It is possible that, due to the increased inertia, the particle orientation is basically affected by the mean shear and the dominating streamwise turbulent intensity. The effect of the streamwise turbulent fluctuations would be to orient the particles with the mean flow direction, and the mean shear would rotate the particle about the spanwise axis. Since it is expected that the turbulent intensities contribute more to the orientation for lighter particles (case F10, F30, F50), it can explain why the orientation of the heavier particles (case S10, S30, S50) seems to be more confined to the xz-plane. Therefore, the heavier particles will be less oriented in the spanwise direction.

Fig. 5(d)–(f) shows the fluctuations in orientation for $\tau^+ = 10$ particles. Also here, the fluctuations become more or less isotropic

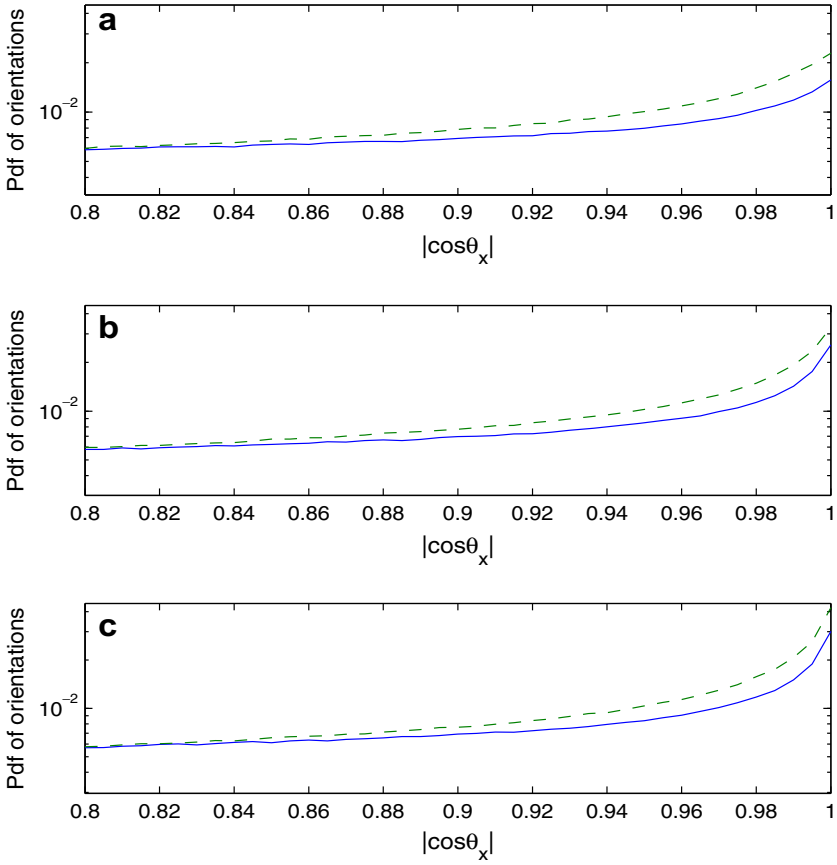

Fig. 6. Pdf of particle streamwise orientations $|\cos\theta_x|$; (—) $\tau^+ = 0.5$, (--) $\tau^+ = 10$. (a) $\lambda = 10$, (b) $\lambda = 30$, and (c) $\lambda = 50$.

away from the near-wall region ($z^+ > 40$). It is seen that the heavier particles fluctuate more in streamwise and wall-normal orientation. The only exception is for S10 particles in the region $z^+ < 7$ where the fluctuations in the streamwise orientation for F10 particles are larger. Anyway, the small fluctuations in spanwise orientation support the idea that the orientation of heavier particles is largely confined to the *xz*-plane.

The previous results that ellipsoidal particles have preferred orientations in the streamwise direction are in agreement with the results of Zhang et al. (2001). They only considered ellipsoids of aspect ratio $\lambda = 5$ and equivalent response time $\tau^+ = 2.26$ in the near-wall region (viscous sublayer, buffer layer). Here, we have used the same mathematical formulation of the particles and a slightly different numerical approach. Also, we have investigated a wider particle parameter space and showed results for the whole turbulent wall layer. It is evident that both the aspect ratio and equivalent response time are important parameters for the orientational behavior of prolate ellipsoids. The results show that streamwise orientation increases with increasing particle length for fixed particle diameters. Newsom and Bruce (1998) stated that the horizontal orientation was more sensitive to fiber diameter than to fiber length. Assuming that Eq. (5) holds for their fibers, the tendency of horizontal orientations increases with increasing inertia. This is exactly what the present results show. Fig. 6 shows a close up of the probability curves for the streamwise orientation in Figs. 2 and 4. It is seen that higher inertia particles have higher probability of orienting in the streamwise direction for a fixed diameter. Hence, in the present case, the increased inertia for fixed particle diameters contributes to the higher probability of streamwise alignment.

5. Conclusions

Direct numerical simulation has been conducted in order to study the orientation of ellipsoidal particles in a turbulent channel flow. It was assumed that the particles were smaller than the Kolmogorov scales at a frictional Reynolds number of 360. The creeping flow versions of the drag force and torque were applied in the particle equations of motion. Six different particle cases with varying aspect ratios and particle equivalent response times were studied. Results show that, in the near-wall region, prolate ellipsoids tend to orient in the mean flow direction. This effect becomes more pronounced with increasing aspect ratio. The effect of increasing particle inertia causes the particle orientation to be more confined to the *xz*-plane. Hence, the heavier particles are less oriented in the spanwise direction. In the core region of the channel, the orientations become isotropic.

Acknowledgements

This work has been supported by The Research Council of Norway through the PETROMAKS programme. The authors would like to thank Professor Goodarz Ahmadi and Roar Meland for helpful discussions. They would also like to thank the reviewers for constructive suggestions.

References

Brenner, H., 1963. The Stokes resistance of an arbitrary particle. Chem. Eng. Sci. 18, 1–25.
Brenner, H., 1964. The Stokes resistance of an arbitrary particle-IV, arbitrary fields of flow. Chem. Eng. Sci. 19, 703–727.
Fan, F.G., Ahmadi, G., 1995. A sublayer model for wall-deposition of ellipsoidal particles in turbulent streams. J. Aerosol Sci. 26, 813–840.
Gallily, I., Cohen, A.H., 1979. On the orderly nature of the motion of nonspherical aerosol particles. II. Inertial collision between a spherical large droplet and axially symmetrical elongated particle. J. Colloid Interface Sci. 68, 338–356.
Gillissen, J.J.J., Boersma, B.J., Mortensen, P.H., Andersson, H.I., 2007. On the performance of the moment approximation for the numerical computation of fiber stress in turbulent channel flow. Phys. Fluids 19, 035102.
Goldstein, H., 1980. Classical Mechanics, second ed. Addison-Wesley Publishing Company.
Harper, E.Y., Chang, I.D., 1968. Maximum dissipation resulting from lift in a slow viscous shear layer. J. Fluid Mech. 33, 209–225.
Jeffery, G.B., 1922. The motion of ellipsoidal particles immersed in a viscous fluid. Proc. Royal Soc. 102, 161–179.
Kuerten, J.G.M., 2006. Subgrid modeling in particle-laden channel flow. Phys. Fluids 10, 025108.
Kulick, J.D., Fessler, J.R., Eaton, J.K., 1994. Particle response and turbulence modification in fully developed channel flow. J. Fluid Mech. 227, 109–134.
Lin, J., Shi, X., Yu, Z., 2003. The motion of fibers in an evolving mixing layer. Int. J. Multiphase Flow 29, 1355–1372.
Marchioli, C., Picciotto, M., Soldati, A., 2007. Influence of gravity and lift on particle velocity statistics and transfer rates in turbulent vertical channel flow. Int. J. Multiphase Flow 33, 227–251.
Newsom, R.K., Bruce, C.W., 1994. The dynamics of fibrous aerosols in a quiescent atmosphere. Phys. Fluids 6, 521–530.
Newsom, R.K., Bruce, C.W., 1998. Orientational properties of fibrous aerosols in atmospheric turbulence. J. Aerosol Sci. 29, 773–797.
Parsheh, M., Brown, M.L., Aidun, C.K., 2005. On the orientation of stiff fibres suspended in turbulent flow in a planar contraction. J. Fluid Mech. 545, 245–269.
Shapiro, M., Goldenberg, M., 1993. Deposition of glass fiber particles from turbulent air flow in a pipe. J. Aerosol Sci. 24, 65–87.
Zhang, H., Ahmadi, G., Fan, F-G., McLaughlin, J.B., 2001. Ellipsoidal particles transport and deposition in turbulent channel flows. Int. J. Multiphase Flow 27, 971–1009.